Available online at http://www.journalijdr.com

IJDR

ISSN: 2230-9926

International Journal of Development Research
Vol. 11, Issue, 11, pp. 52101-52107, November, 2021
https://doi.org/10.37118/ijdr.23382.11.2021

RESEARCH ARTICLE

OPEN ACCESS

TEMPERATURE DISTRIBUTION ANALYSIS IN THE THERMAL ABSORBER OF AN INDIRECT SOLAR DRYER

Brenda Fernandes Ribeiro[1,*] and Antonio Gomes Nunes[2]

[1] Bachelor in Science and Technology from Universidade Federal Rural do Semi-Árido (UFERSA), Mossoró, RN, Brasil

[2]PhD in Process Engineering fromUniversidade Federal de Campina Grande (UFCG).Professor at Universidade Federal Rural do Semi-Árido (UFERSA). Mossoró, RN, Brasil

ARTICLE INFO

Article History:

Received 14th August, 2021
Received in revised form
26th September, 2021
Accepted 11th October, 2021
Published online 30th November, 2021

Key Words:

Solar Dryer, Heat Conduction,
Mathematical Modeling,
Partial Differential Equations.

****Corresponding author:***
Brenda Fernandes Ribeiro

ABSTRACT

This article proposes a mathematical modeling for the temperature distribution along a surface. The model was developed based on the Fourier's law of heat conduction and tested on empirical data obtained in 9 days of experiments performed on an indirect exposure solar dryer at UFCG (Campina Grande, PB, Brazil). The initial condition was considered position-dependent and the boundary conditions were considered position and time-dependent, as well as the heat generation equation added to the model to include the effects of solar irradiation. The application of Fourier's law of conduction resulted in a non-homogeneous partial differential equation, which was solved using the eigenfunction expansion method. The comparison between 27 experimental data and the equivalent data obtained through the model revealed an average percentage error of 2.17% for all temperature data given in Kelvin.

Citation: ***Brenda Fernandes Ribeiro and Antonio Gomes Nunes.*** "Temperature distribution analysis in the thermal absorber of an indirect solar dryer*", International Journal of Development Research*, 11, (11), 52101-52107.

INTRODUCTION

The applications of clean, accessible and renewable energy sources represent a key role in promoting sustainable development. In this bias, Nunes (NUNES, 2016) proposed the study of an indirect solar dryer with vast potential of use, mainly in the fruitful sector. The prototype built and studied (NUNES, 2016) efficiently dried the silver bananas (*Musa spp.*) and operated through photovoltaic and thermal solar energy. Four experiments were performed, the first one lasted three days and the three others lasted two days, totaling nine days of data collection. The data has been collected from 8:00 a.m. to 4:00 p.m. Temperature and solar irradiation data were recorded every hour of experiment. The present article intends to investigate, through the development of a mathematical model and based on the collected data, how the transfer of heat by conduction occurs through the plate that works as thermal absorber in the solar dryer prototype (NUNES, 2016). The analyzed solar collector has as absorber a fibrocement tile painted in matte black. For the modeling of the problem, the tile was considered a flat plate with one-dimensional conduction. The temperature and solar irradiation experimental data were used in the elaboration of a non-homogeneous partial differential equation with time-dependent boundary conditions and position-dependent initial condition. In order to include the effects of solar irradiation, a time-dependent thermal energy generation equation was formulated. The non-homogeneous partial differential equation was solved through the eigenfunction expansion technique – analogous to the method of variation of parameters applied in ordinary differential equations (FARLOW, 1982). The solution obtained was given by a Fourier series. For the graphic plotting of the resolution, performed in Mathematica software, the thirty first terms of the series were considered. The mean percentage error calculated for the temperature data –in Kelvin – was 2.71%.

MATHEMATICAL MODEL

Prototype and experiments: The fundamental parts of the indirect solar dryer built by Nunes and tested experimentally in the drying of fruits (silver bananas) are: solar collector - object of study in the present article -, drying chamber and data measurement system. Figure 1 shows a top view of the prototype with indication of each component.

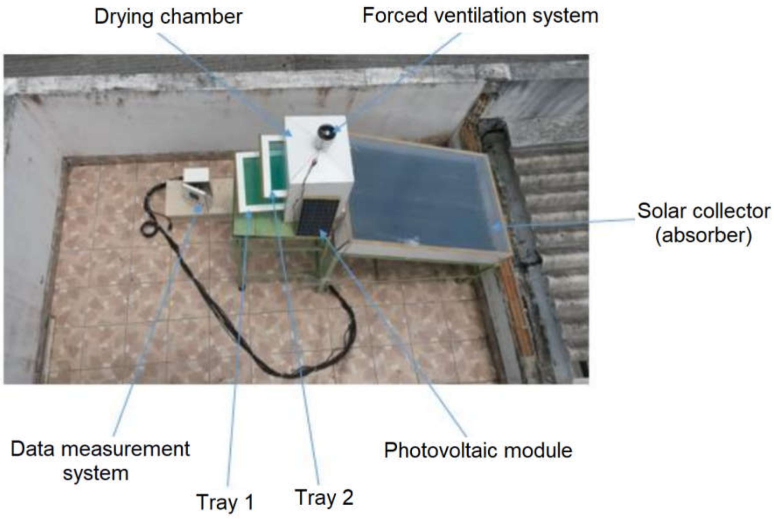

Figure 1. Top view of the prototype with indication of each component (1).

The tests with the prototype were carried out at the Experimental Laboratory of Thermal Machines (LEMT) in the Federal University of Campina Grande (UFCG), located in the city of Campina Grande in the state of Paraíba, Brazil. Four experiments were carried out on drying of silver bananas, the first one occurred in three days, with a total duration of 24 hours (8 hours per day), and the three other experiments were performed in two days, with a total duration of 16 hours each. Empirical data were collected on March 12-14; March 26-27; April 28-29; and May 26-27, in the year of 2015, from 8:00 a.m. to 4:00 p.m. each day (NUNES, 2016). Ten thermocouples were used to collect the temperature data, six of which were distributed in the solar collector and four in the drying chamber. The data of solar irradiation were obtained through the LEMT/UFCG weather station (NUNES, 2017) – model HD32MT.1, SN 11031486 and FW 0714141114. Data of mass variations of bananas and data related to humidity and air velocity were also collected.

Heat conduction axis and tile shape considerations: The solar dryer prototype (Figure 2-a) built and studied by Nunes in his thesis is composed by a medium-density fiberboard (MDF) tray, a black-painted fibrocement roof tile of dimensions 0.7 x 1.25 m and a polycarbonate cover (NUNES, 2016). The tray (Figure 2-b) and the polycarbonate cover imply the isolation of the tile in two axes. Therefore, it is appropriate to consider that temperature variations are most significant along the X-axis (Figure 2-b), due to the air inlet and outlet openings of the tray. By considering one-dimensionalheat conduction, it is possible to approximate – for thermal analysis purposes – the tile as being a flat plate –instead of wavy shaped.

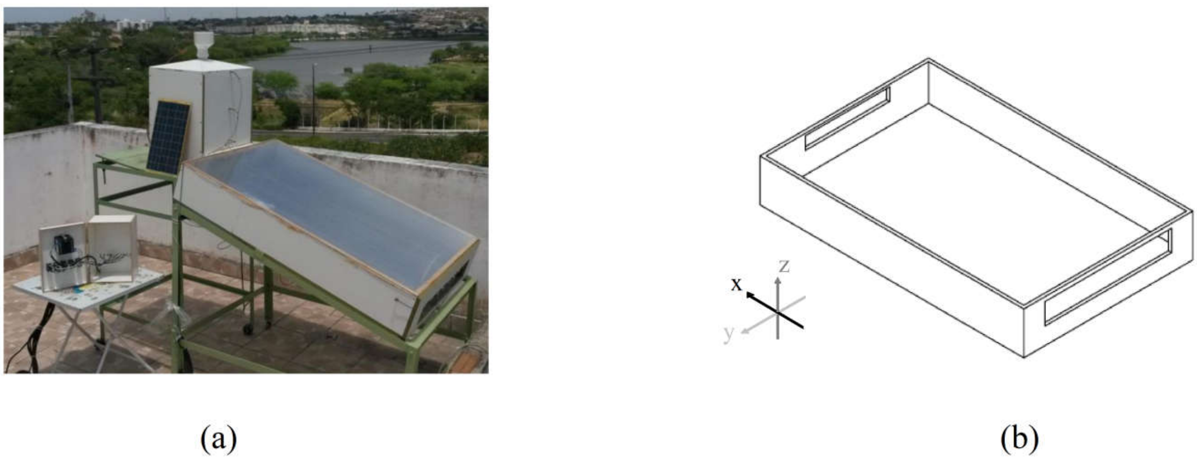

Figure 2: (a) Solar dryer prototype built and studied by Nunes (2016) (b) Schematic drawing of the tray that composes the solar collector of the prototype (Adapted from (1))

The validation of the one-dimensional conductivity consideration is possible through the analysis of the empirical data collected: the thermocouples distributed along the Y-axis on the tile surface showed – at the same moment of measurement – temperature variations much lower than those observed in the thermocouples distributed along the X-axis. Figure 3 shows the distribution of the thermocouples used in the experiments and the measured temperatures in the solar dryer collector for one day of experiment. The collected data reveal that the temperature differences between the Tp5 and Tp6 thermocouples – which are at approximately the same position along the X-axis with variation in Y-axis – are considerably smaller than the variations observed in the thermocouples that have same position along the Y-axis – with position variation in the X-axis –: Tp2, Tp4 and Tp5 for a long period of experiment. Figure 3: (a) Indication the solar dryer parts and distribution of the thermocouples used in the experiments.

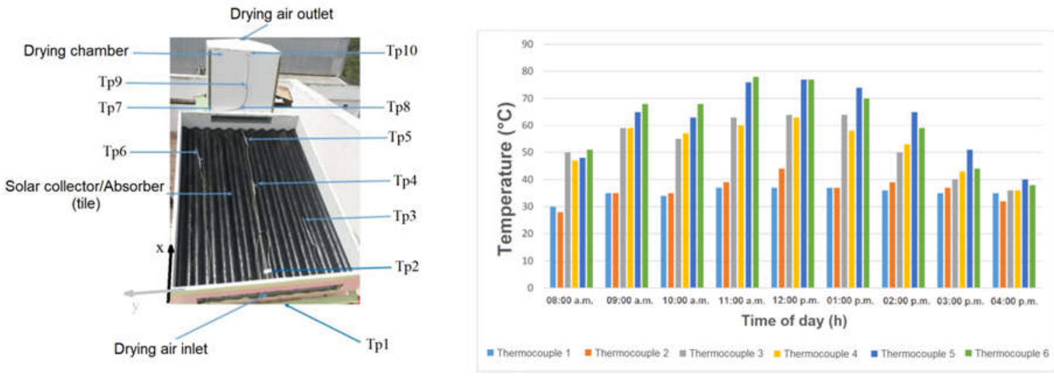

(a) (b)

Figure 3. (a) Indication the solar dryer parts and distribution of the thermocouples used in the experiments. (b) Graph of the temperature distribution in the solar collector for an experimental test day (03/26/2015) (1)

Heat conduction equation: The Fourier law of heat conduction stablishes that the rate of heat flow($\dot{Q}$) is proportional to the gradient of temperature and to the areal normal to the flow direction (A) (ÇENGEL, 2012) – given in m^2. For unidimensional conduction through X-axis:

$$\dot{Q} = -kA\frac{dT}{dx} \tag{1}$$

Where k (W/m·K) is a proportionality constant called *thermal conductivity* that varies according to the material (5).

For a single dimensional conduction with constant thermal conductivity and heat generation rate ($\dot{e}_{gen}$) on the plate, the equation in rectangular coordinates is given by:

$$\frac{\partial T}{\partial t} = \alpha\left(\frac{\partial^2 T}{\partial x^2} + \frac{\dot{e}_{gen}}{k}\right) \tag{2}$$

Where α is the *thermal diffusivity* of the material, given by the quotient of the conductivity for the product between *density* and *specific heat:* $k/(\rho \cdot c)$.

For developing the partial differential equation referent to the studied case, the heat generation was considered a time-dependent function, as well as the boundary conditions. All the equations were formulated based on thecollected experimental data (NUNES, 2016). The constants*k, ρ* and *c* for the fibrocement – material that composes the roof tile to be analyzed – were extracted from the Brazilian norm NBR15220 (6).

Formulation of the initial condition, boundary conditions and energy generation equations

The partial differential equation (PDE) of the modeling problem is given by:

$$\frac{\partial T(x,t)}{\partial t} = \alpha\frac{\partial^2 T(x,t)}{\partial x^2} + E(t) \tag{3}$$

In which the thermal diffusivity isα= 0.0005952 m^2/s (ABNT, 2005) and *E(t)* correspondsto que thermal energy generation equation on the absorber (tile), developed to include the solar irradiation effects.The function *E(t)*is directly proportional to the solar irradiation– variant over time –*I(t)* and to the collector efficiencyε. *E(t)* is inversely proportional to the fibrocement density and specific heat – for this is the material that composes the roof tile. Therefore, wehave:

$$E(t) = \frac{1}{\rho c} \cdot \varepsilon \cdot I(t) \tag{4}$$

For the fibrocement density, the valueρ= 1900kg/m^3 (6) was adopted.The specific heat of the fibrocement was considered$c$ = 0.84J/kg□K (ABNT, 2005). The adopted value for the collector's efficiencyε = 19.89%considered the average of the efficiency values obtained for each experiment performed (NUNES, 2016). The elaboration of the irradiation function *I(t)*was based on the average irradiation data collected each hour during the nine days of experiment (Table 1). In the function, the measurement unit for irradiation is W/$m^2$and the time is measured in seconds. The time of day in which the experiments started was considered as the function's "initial time" (8:00 a.m.). The quadratic equation*I(t)*is given by Equation 5,which has coefficient of determination (R^2) equal to 0.975. That indicates a great approximation between the function values and the empirical data.

$$I(t) = -2 \cdot 10^{-6} \cdot t^2 + 0.0604 \cdot t + 547.9 \tag{5}$$

By replacing the values of theρ, c andεconstants and the function*I(t)*, we have:

$$E(t) = \frac{1}{1900 \cdot 0.84} \cdot 0.1989 \cdot (-2 \cdot 10^{-6} \cdot t^2 + 0.0604 \cdot t + 547.9) \tag{6}$$

Table 1. Processing of the solar irradiation experimental data

Time (s)	Solar Irradiation(W/m^2)									
	DAY 1	DAY 2	DAY 3	DAY 4	DAY 5	DAY 6	DAY 7	DAY 8	DAY 9	AVERAGE
0	400	430	675	680	575	675	670	370	430	545.000
3600	780	595	820	830	850	830	840	450	780	752.778
7200	980	790	720	720	1020	725	725	565	920	796.111
10800	980	1000	1000	1010	1050	1010	1005	810	900	973.889
14400	985	1000	980	970	950	980	980	750	660	917.222
18000	760	670	950	920	650	925	930	800	720	813.889
21600	820	420	780	775	650	780	780	410	630	671.667
25200	590	460	600	600	520	600	610	300	580	540.000
28800	225	225	260	270	240	270	260	200	190	237.778

The boundary conditions equations were developed through the analysis and processing of the thermocouples Tp1 and Tp7 temperature data, which correspond, respectively, to the absorber air input (ambient temperature) and output (drying chamber input temperature). Cubic functions with satisfactory coefficients of determination were generated. The Table 2 relates the data applied in the formulation of the boundary equations $T_1(t)$ – developed through Tp1 collected data – and $T_2(t)$ – developed through Tp7 collected data – which consist with the input and output temperature of the air that passes through the prototype's solar collector.

Table 2: Empirical data processing for boundary conditions development

BOUNDARY CONDITION: AIR INPUT(Tp1)										
Time (s)	Temperature(°C)									AVERAGE TEMPERATURE (K)
	DAY 1	DAY 2	DAY 3	DAY 4	DAY 5	DAY 6	DAY 7	DAY 8	DAY 9	
0	27	28	29	30	27	29	26	29	27	301.15
3600	32	31	34	35	34	33	32	31	33	305.9278
7200	33	32	35	34	35	34	34	34	34	307.0389
10800	34	35	36	37	35	37	35	35	36	308.7056
14400	36	35	36	37	35	37	35	34	36	308.8167
18000	35	35	35	37	36	37	36	35	37	309.0389
21600	35	34	35	36	35	36	37	36	38	308.9278
25200	33	34	–	35	35	34	36	35	38	308.15
28800	33	34	33	35	34	–	36	–	36	307.5786
BOUNDARY CONDITION: AIR OUTPUT (Tp7)										
Time (s)	Temperature (°C)									AVERAGE TEMPERATURE (K)
	DAY 1	DAY 2	DAY 3	DAY 4	DAY 5	DAY 6	DAY 7	DAY 8	DAY 9	
0	34	30	40	41	33	38	31	39	36	308.9278
3600	46	45	49	52	46	47	42	46	54	320.5944
7200	51	42	52	52	56	50	48	47	55	323.4833
10800	52	55	53	58	57	53	52	58	52	327.5944
14400	50	55	55	59	55	55	55	52	48	326.9278
18000	45	49	51	57	52	48	46	54	52	323.5944
21600	40	43	46	50	52	42	46	41	52	318.9278
25200	37	37	38	43	44	37	45	38	46	313.7056
28800	34	39	47	37	38	–	37	–	37	311.5786

Notice: The missing data has been suppressed for it has not been collected or has presented unusual and highly discrepant values.

The polynomial functions $T_1(t)$ and $T_2(t)$ are given by equations 7 and 8. The coefficients of determination are, respectively, equal to 0.977 e 0.982. In both equations, the temperature is measured in Kelvin and the time in seconds.

$$T_1(t) = 8 \cdot 10^{-13} \cdot t^3 - 6 \cdot 10^{-8} \cdot t^2 + 0.0012 \cdot t + 301.51 \quad (7)$$

$$T_2(t) = 3 \cdot 10^{-12} \cdot t^3 - 2 \cdot 10^{-7} \cdot t^2 + 0.0037 \cdot t + 309.04 \quad (8)$$

The initial condition equation$\varphi(x)$ consists in a quadratic function defined by the relation between the X-axis position (distance from the air input) and the average initial temperature$\varphi$of the thermocouples Tp2, Tp4 and Tp5 for the nine days of experiment (Table 3 **Erro! Fonte de referência não encontrada.**).

Table 3. Initial condition data

THERMOCOUPLE	AVERAGE TEMPERATURE AT t = 0s (Kelvin)	DISTANCE FROM THE AIR INPUT (m)
Tp2	302.5944	0
Tp4	314.9278	0.63
Tp5	314.4833	0.84

For it is a quadratic function formulated through three points, the function $\varphi(x)$, which is given by Equation 9, has $R^2 = 1$.

$$\varphi(x) = -25.825 \cdot x^2 + 35.847 \cdot x + 30;\quad (9)$$

2.5. Mathematical model and partial differential equationresolutionmethod

The proposed mathematical modeling consists, thus, of a flat plate measuring L = 1.25 m (length) with one-dimensional conduction trough the X-axis (Equation 3), boundary conditions given by $T_1(t)$ (Equation 7) and$T_2(t)$ (Equation 8), initial condition$\varphi(x)$ (Equation 9) and thermal energy generation$E(t)$ (Equation 6). The Figure 4schematically illustrates the modeling.

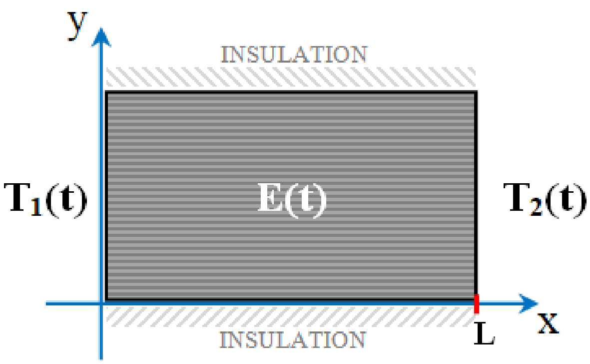

Figure 4. Schematic drawing of the modeling

The formulated partial differential equation is non-homogeneous due to the consideration of thermal energy generation in the tile. Furthermore, the boundary conditions are likewise non-homogeneous, for they are not null. For solving this equation, another differential equation has been generated, associated to the original one, but with homogeneous boundary conditions. For that, the $T(x,t)$ function as been decomposed as the sum of a steady-state equation $S(x,t)$ and a transient state equation $U(x,t)$:

$$T(x,t) = S(x,t) + U(x,t) \quad (10)$$

The steady-state equation is given by:

$$S(x,t) = T_1(t) + \frac{x}{L} \cdot [T_2(t) - T_1(t)] \quad (11)$$

Thus, the $T(x,t)$ function can be written as:

$$T(x,t) = T_1(t) + \frac{x}{L} \cdot [T_2(t) - T_1(t)] + U(x,t) \quad (12)$$

Therefore:

$$U(x,t) = T(x,t) - \left\{T_1(t) + \frac{x}{L} \cdot [T_2(t) - T_1(t)]\right\} \quad (13)$$

For$U$ (t,x) the boundary conditions are null:

$$U(0,t) = U(L,t) = 0 \quad (14)$$

Hence, the new differential equation with homogeneous boundary conditions is given by:

$$\frac{\partial U}{\partial t} = \alpha \frac{\partial^2 U}{\partial x^2} + E(t) - \frac{\partial S}{\partial t} \quad (15)$$

The initial condition is:

$$U(x,0) = \varphi(x) - S(x,0) \quad (16)$$

The new equation can be solved through the eigenfunction expansion method, which is analogous to the variation of parameters method applied to non-homogeneous ordinary differential equations (2), as both methods part from the solution of the homogeneous equation associated to the non-homogeneous one. In the presented case, the associated homogeneous equation is given by Equation 17.

$$\frac{\partial U}{\partial t} = \alpha \frac{\partial^2 U}{\partial x^2} \quad (17)$$

By applying the separation of variables method (7), for $U(x,t) = X_n(x)\square\Gamma_n(t)$, we have:

$$X_n(x) = \sin\left(\frac{n\pi x}{L}\right) n = 1, 2, 3 \ldots \quad (18)$$

To determine $\Gamma_n(t)$, an$f_n(t)$function is supposed for that the non-homogeneous partof the PDE is given by:

$$E(t) - \frac{\partial S}{\partial t} = F(x,t) = \sum_{n=1}^{\infty} f_n(t) \cdot \sin\left(\frac{n\pi x}{L}\right) \quad (19)$$

Multiplying both sides by $X_n(x)$ and integrating in x from 0 to L, $f_n(t)$ is obtained:

$$f_n(t) = \frac{2}{L} \cdot \int_0^L F(x,t) \cdot \sin\left(\frac{n\pi x}{L}\right) \cdot dx \quad (20)$$

Expanding the differential equation with the obtained terms, we have:

$$\frac{\partial U}{\partial t} - \alpha \frac{\partial^2 U}{\partial x^2} - F(x,t) = 0 \quad (21)$$

$$\sum_{n=1}^{\infty} X_n(x) \cdot \frac{\partial \Gamma_n(t)}{\partial t} - \alpha \sum_{n=1}^{\infty} \frac{\partial^2 X_n(x)}{\partial x^2} \cdot \Gamma_n(t) - \sum_{n=1}^{\infty} f_n(t) \cdot X_n(x) = 0 \quad (22)$$

Therefore,

$$\sum_{n=1}^{\infty} \left[\frac{\partial \Gamma_n(t)}{\partial t} + \alpha \left(\frac{n\pi}{L}\right)^2 \cdot \Gamma_n(t) - f_n(t)\right] \cdot X_n(x) = 0 \quad (23)$$

As $X_n(x)$ is not null for every x, we have, on Equation 23, an ODE that can be solved to determine $\Gamma_n(t)$. The initial value problem (IVP) for solving the ODE is determined by developing the Equation 16 – similarly to what has been done with Equation 19. The initial condition $\Gamma_n(0)$ is given by Equation 24.

$$\Gamma_n(0) = \frac{2}{L} \cdot \int_0^L [\varphi(x) - S(x,0)] \cdot \sin\left(\frac{n\pi x}{L}\right) \cdot dx \quad (24)$$

By solving the IVP presented in Equation 24, we have:

$$\Gamma_n(t) = \left[\frac{2}{L} \cdot \int_0^L [\varphi(x) - S(x,0)] \cdot \sin\left(\frac{n\pi x}{L}\right) \cdot dx\right] \cdot e^{-\left(\frac{n\pi}{L}\right)^2 \cdot \alpha \cdot t} + \left[\int_0^t e^{\left(\frac{n\pi}{L}\right)^2 \cdot \alpha \cdot \tau} \cdot f_n(\tau) \cdot d\tau\right] \cdot e^{-\left(\frac{n\pi}{L}\right)^2 \cdot \alpha \cdot t} \quad (25)$$

The final result, in terms of the primary equations $T_1(t)$, $T_2(t)$, $\varphi(x)$, $E(t)$ and the constants L and α, is given by the Fourier series expressed in Equation 26.

$$T(x,t) = T_1(t) + \frac{x}{L} \cdot [T_2(t) - T_1(t)] + \sum_{n=1}^{\infty} \left\{\frac{2}{L} \cdot \int_0^L \left\{\varphi(x) - \left\{T_1(0) + \frac{x}{L} \cdot [T_2(0) - T_1(0)]\right\}\right\} \cdot \sin\left(\frac{n\pi x}{L}\right) \cdot dx\right\} \cdot e^{-\left(\frac{n\pi}{L}\right)^2 \cdot \alpha \cdot t} \cdot \sin\left(\frac{n\pi x}{L}\right) + \sum_{n=1}^{\infty} \left\{\int_0^t e^{\left(\frac{n\pi}{L}\right)^2 \cdot \alpha \cdot \tau} \cdot \left\{\frac{2}{L} \cdot \int_0^L \left[-\frac{dT_1(\tau)}{d\tau} - \frac{x}{L} \cdot \frac{dT_2(\tau)}{d\tau} + \frac{x}{L} \cdot \frac{dT_1(\tau)}{d\tau} + E(\tau)\right] \sin\left(\frac{n\pi x}{L}\right) \cdot dx\right\} \cdot d\tau\right\} \cdot e^{-\left(\frac{n\pi}{L}\right)^2 \cdot \alpha \cdot t} \cdot \sin\left(\frac{n\pi x}{L}\right) \quad (26)$$

Graphic representation of the solution and comparison to the experimental data: For the graphic representation of the obtained solution – the function $T(x,t)$ – the first thirty terms of the series were considered, which means that the n contained in Equation 26 varied from 1 to 30. Because the thermal absorber (roof tile) had passed through heating followed by cooling process during each day of experiment, two graphs were developed to avoid overlapping of the curves. Both graphs contain the representations of temperature depending on position for each hour of experiment. The position reference is the drying air input ($x=0$). The heating of the roof tile (Figure 5-a) occurred along the first four hours of experiment, from 8:00 a.m. to 12:00 p.m., which equals to $0 \leq t \leq 4h$, for the time reference is set to the beginning of the experiment. The cooling period (Figure 5-b) happened during the final hours of the experiment, from 12:00 p.m. to 4:00 p.m., that is, for $5h \leq t \leq 8h$.

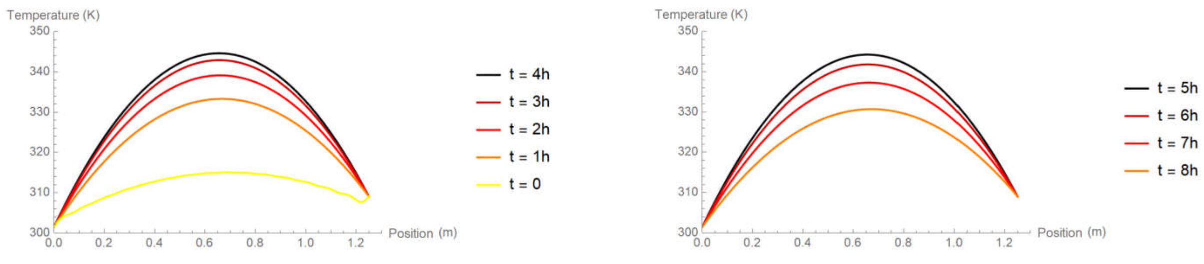

(a) (b)

Figure 5. Graphs of temperature (K) in function of position (m) plotted with Mathematica software for the periods of (a) heating and (b) cooling of the roof tile

The average percentage error $\epsilon_{\%}$ was obtained trough Equation 27:

$$\epsilon_{\%} = 100\% \cdot \frac{\sum_{n=1}^{27} |T_n - T_n|}{27} \quad (27)$$

In which T_n corresponds to the n-esimal temperature value found trough the function $T(x,t)$ for the same position x and time t as the empirical value $T_{n\,exp.}$. For there were considered temperatures in nine distinct moments for each thermocouple analyzed (Tp2, Tp4 e Tp5), n varies from 1 to 27 – this n term is not the same as the one presented in Equation 26. The average percentage error is 2.71%, with values that vary from 0.002% to 6.25% among the 27 data analyzed. All the values were evaluated considering the temperatures in Kelvin.

CONCLUSION

The mathematical modeling proposed in the present article has properly presented the thermal distribution on the surface of a thermal absorber (collector) of an indirect exposure solar dryer. The percentage error obtained for the empirical data (NUNES, 2016) was beneath 3%, which means a satisfactory result. The considerations of boundary conditions and heat generation depending on time, as well as the initial condition depending on position, allowed a more in-depth applicability of the model, not only for more diverse meteorological conditions, as for other situations involving heat conduction. For future studies, it is suggested the consideration of other forms of heat transfer (convection and radiation), as well as the inclusion of conduction in two or three axis in order to obtain a better and more precise mathematical model, even more realistic and with lesser percentage error.

REFERENCES

(NUNES, 2016) NUNES, A.G. Desenvolvimento experimental de um secador solar multienergético para secagem de frutas. 2016. 175f. Tese (Doutorado) – Centro de Ciências e Tecnologia, Universidade Federal de Campina Grande – UFCG, Campina Grande – PB, 2016.

FARLOW, S.J. Partial differential equations for scientists and engineers. Wiley, New York: Dover, 1982. 448p.

NUNES, A.G. et al. Experimental Tests on a Solar Dryer of Indirect Exposure Used to Produce Dried Bananas. DefectandDiffusionForum, v. 369, p. 173-176, 2016.

NUNES, A.G.; GRILO, M.B. Desenvolvimento experimental de um secador solar multienergético. 1. ed. Novas Edições Acadêmica, 2017. v. 1. 175p.

ÇENGEL, Y.A. Transferência de Calor e Massa: Uma Abordagem Prática, 4ª Edição, Editora McGrawHill, 2012.

Associação Brasileira de Normas Técnicas (ABNT). NBR 15220-2: Desempenho Térmico de Edificações - parte 2: Métodos de cálculo da transmitância térmica, da capacidade térmica, do atraso térmico e do fator solar de elementos e componentes de edificações. Rio de Janeiro, 2005.

ZILL, D.G.; CULLEN, M.K. Equações diferenciais, vol. 2. São Paulo: Makron Books, 2001. 3ªa ed.

****